J Mater Sci (2008) 43:38–42
DOI 10.1007/s10853-007-2135-3

Defect chemistry of nano-grained barium titanate films

Jon F. Ihlefeld · Mark D. Losego · Ramòn Collazo · William J. Borland · Jon-Paul Maria

Received: 3 March 2007 / Accepted: 29 August 2007 / Published online: 27 September 2007

Abstract Polycrystalline barium titanate thin films have been prepared with 100 ppm of *B*-site acceptor dopants Ca, Mg, and Mn via chemical solution deposition on base metal substrates. The films are fired in low pO_2 atmospheres at 900 °C to prevent substrate oxidation. All dopant species produce low loss, space-charge free material without secondary reoxidation anneals. We note that the dopant concentrations required to compensate for oxygen non-stoichiometry are substantially greater than expected by equilibrium thermodynamic calculations. This observation is rationalized in the context of a composite oxygen defect model with differing reduction enthalpies for grain interiors and surfaces.

As particle and grain dimensions approach the nanometer scale many properties are known to deviate from their bulk reference states. Many of these changes can be related to an overall increase in the surface area to volume ratio. For example, in many oxides the surfaces and interfaces are known to harbor substantially larger point defect densities than the crystal interior, as has been demonstrated in both CeO_2 and TiO_2 [1, 2]. As the dimensions of ferroelectric crystals decrease several well-documented phenomena occur including reduced permittivity and decreased phase transition temperatures [3–6]. Recently, enhanced *p*-type conductivity has been observed in nanocrystalline barium titanate ceramics [7]. It has been suggested that this enhancement results from a change in the overall reduction enthalpy as grain sizes decrease and a subsequent oxygen vacancy concentration increase. This, coupled with oxygen-rich processing environments, results in holes as the dominant charge carrier. In this article, we explore the defect mechanisms potentially responsible for this deviation by investigating the effect of acceptor dopants and reoxidation anneals on the room temperature dielectric properties in $BaTiO_3$ polycrystalline films. A composite defect structure model that accounts for these characteristics is proposed.

The ability to deposit complex oxide thin films on base metal electrodes and use heat treatments similar to those commonly applied to bulk ceramics has recently been demonstrated [8–12]. Practically, this requires low oxygen, partial pressures, and process temperatures greater than 800 °C, and establishes an oxygen point defect concentration problematic from the perspective of insufficient insulation resistance. As a result, many insulating oxides processed under reductive conditions require secondary reoxidation anneals at higher oxygen pressures and lower temperatures to minimize electrically active point defects associated with the intrinsic oxygen non-stoichiometry [13]. To illustrate this, Fig. 1 shows a capacitance–voltage measurement for low pO_2 processed pure $BaTiO_3$ films with and without reoxidation. The necessity of the secondary anneal becomes clear when comparing the high field loss tangents. For a film without a secondary anneal loss tangents exceed

J. F. Ihlefeld · M. D. Losego · R. Collazo · J.-P. Maria
Department of Materials Science and Engineering, North Carolina State University, Raleigh, NC 27695, USA

J. F. Ihlefeld (✉)
The Pennsylvania State University, University Park, PA 16802, USA
e-mail: jfi2@psu.edu

W. J. Borland
DuPont Electronic Technologies, Research Triangle Park, NC 27709, USA

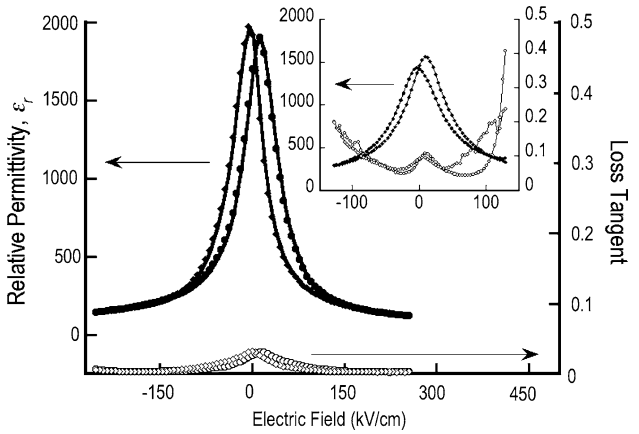

Fig. 1 Field dependence of permittivity (solid markers) and loss tangent (open markers) for a 600 nm thick $BaTiO_3$ film after a reoxidation anneal. Inset shows the field dependence without reoxidation

0.4 (40%) at fields less than 150 kV/cm. Alternatively, a film reoxidized under the proper conditions yields loss tangents less than 0.003 (0.3%) at fields in excess of 250 kV/cm. In many cases, the relative permittivity and tunability also improve, likely due to a decrease in point defects that pin domain wall motion.

As an alternative to secondary anneals, acceptor dopants can be incorporated and the intrinsic oxygen vacancies formed from processing can be balanced by largely immobile aleovalent dopant ions rather than comparatively mobile electrons. When properly done, this type of ionic compensation is consistent with low loss tangent, large insulation resistance values, and excellent reliability [14–18]. The present work demonstrates the use of Mn, Mg, and Ca as acceptor dopants on the $BaTiO_3$ lattice *B*-site. In this study, Ba:Ti cation ratios were controlled at the ppm level to persuade dopant site occupancy and ensure that cation ratio did not predominate compensation. The results are discussed in context of the defect chemistry in reduced barium titanate and the effect of fine grain size on the measured properties.

Films were formed using a chemical solution deposition approach with a chelate chemistry as has been outlined in previous work [10, 11]. 0.3 molar barium titanate stock solutions were synthesized with a 100 ppm titanium deficiency. Separate dilute dopant precursor solutions were prepared by dissolving the acetate hydrates of the metal ions in either acetic acid or a solution composed of methanol, diethanolamine, triethanolamine, and nitric acid. The dopant solutions were approximately 0.042M. A digital microbalance was used to measure and control stoichiometry to approximately a 10 ppm level. Films were spin cast onto 18 μm thick bare copper foils in 6 layers with a 250 °C hot plate dry and gel consolidation anneal separating coatings. The final post-fired film thickness was 600 nm. The gel/foil stack was then fired in a low pO_2 atmosphere composed of hydrogen, water vapor, and N_2 carrier at 900 °C for 30 min prior to cooling to room temperature in the same gas composition. An oxygen partial pressure consistent with copper reduction and barium titanate oxidation was measured in situ at 900 °C to be 5×10^{-13} atm [19]. Metal-insulator-metal capacitor structures were defined using shadow masks and RF magnetron sputtered Pt top electrodes. Field dependent dielectric measurements were conducted at 10 kHz with a 0.8 kV/cm oscillator. Frequency dependent measurements used identical oscillator amplitudes and zero DC bias.

Figure 2 shows X-ray diffraction data revealing no secondary or interfacial copper oxide phases with only perovskite barium titanate peaks present, consistent with previous studies [10, 11]. Plan-view and cross-sectional microstructural characterization by field-emission scanning electron microscopy (FE-SEM) revealed dense films, 125 nm average grain diameters, and constant grain size with and without dopants within the concentration range investigated as shown in Fig. 3.

For each dopant type, the 100 ppm acceptor levels were sufficient to form insulating material with high-field loss tangents below 0.01 (1%). Representative field dependent data for a Mg-doped film is shown in Fig. 4. Analogous trends were identified for Ca and Mn. Tunability values in the range of 8:1 and low-field permittivity values near 2,000 are maintained in all cases. Figure 5 shows the frequency dependent dielectric response for (a) an undoped as-fired film, (b) an undoped reoxidized film, and (c) a Mg doped as-fired film. No permittivity dispersion or loss peaks representative of space charge contributions are present in the reoxidized or doped films. In the undoped as-fired film, however, a strong loss tangent space charge contribution is evident [20]. The similar doped and reoxidized results suggest that electronic compensation of

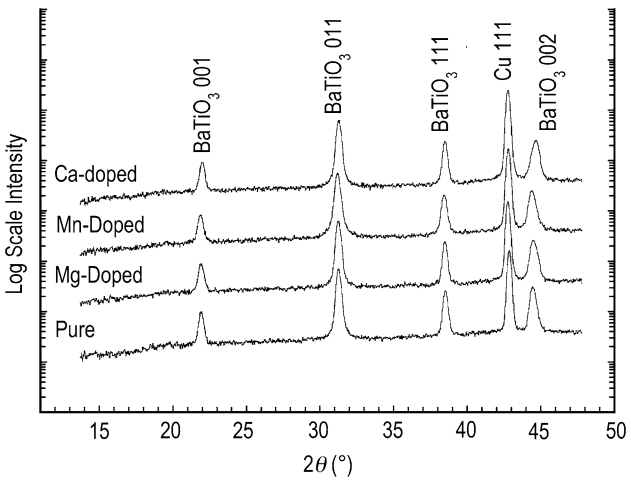

Fig. 2 θ-2θ X-ray diffraction patterns for pure and doped $BaTiO_3$ thin films on copper substrates

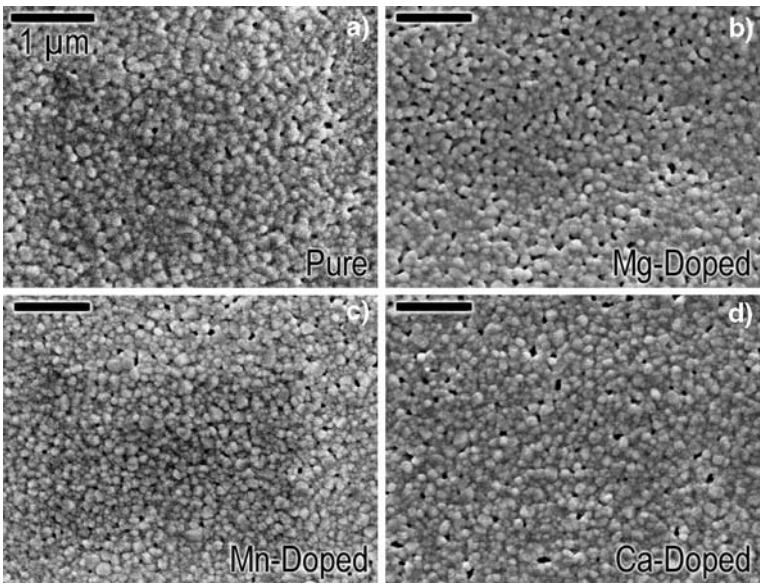

Fig. 3 FE-SEM images of (**a**) pure $BaTiO_3$, (**b**) 100 ppm Mg-doped $BaTiO_3$, (**c**) 100 ppm Mn-doped $BaTiO_3$, and (**d**) 100 ppm Ca-doped $BaTiO_3$

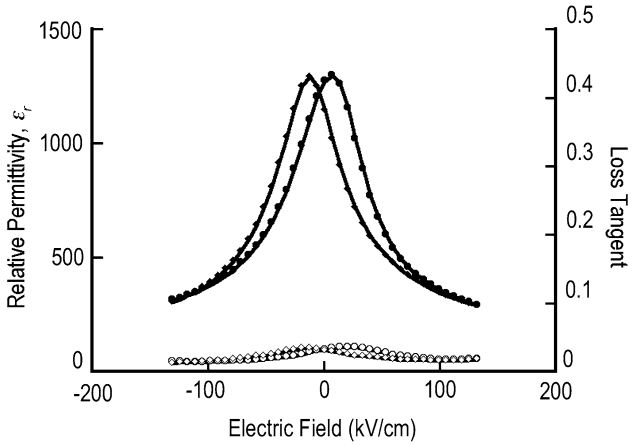

Fig. 4 Field dependence of permittivity (solid markers) and loss tangent (open markers) for a 600 nm thick $BaTiO_3$ film doped with 100 ppm Mg on the perovskite *B*-site fired at 5×10^{-13} atm O_2

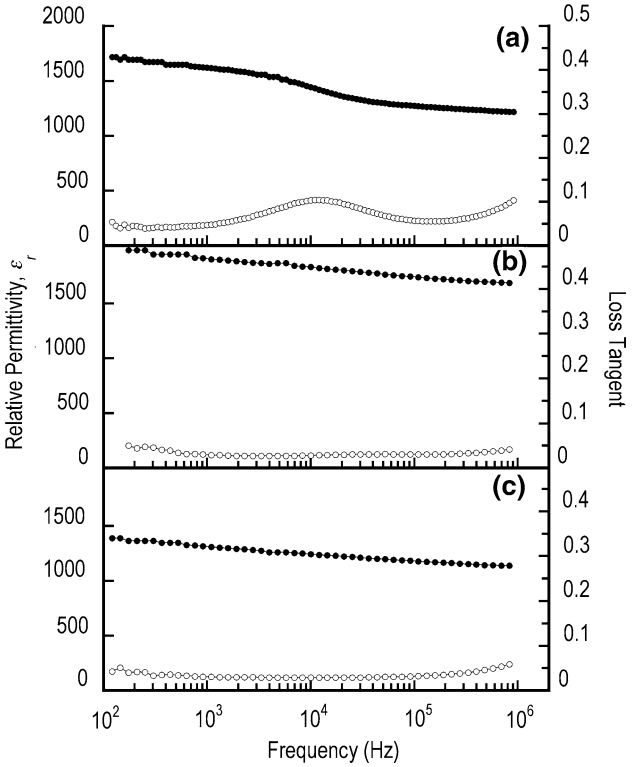

Fig. 5 Frequency dependence of permittivity (solid markers) and loss tangent (open markers) for (**a**) pure $BaTiO_3$ without reoxidation, (**b**) pure $BaTiO_3$ with reoxidation, and (**c**) 100 ppm Mg doped $BaTiO_3$, all fired at 5×10^{-13} atm O_2

oxygen vacancies is responsible for the high loss values and strong dispersion in the undoped as-fired state. All acceptor dopants shift the conductivity minimum toward lower pO_2 processing conditions and chemical precursors contain numerous impurities at the ppm levels of present interest [21–23]. The chemical assays for the precursor materials reveal approximately 50 ppm acceptor ions. However, a similar level of donor impurities is also identified and these two dopant populations should compensate resulting in a small intrinsic carrier level. Unfortunately, the thin layers and small sample sizes preclude sufficiently sensitive post-processing impurity level measurements.

To determine if the doping level used is appropriate for ionic compensation, films from the same as-cast gels were processed under higher pO_2 conditions of 5×10^{-11} atm - a level still within the copper-barium titanate phase stability window. Conceptually, if the dopant quantity is just right, annealing in a slightly higher pO_2 will produce fewer oxygen vacancies, there will be too many cation acceptors, and holes will be created to achieve electroneutrality. Voltage and frequency dependence of permittivity and loss

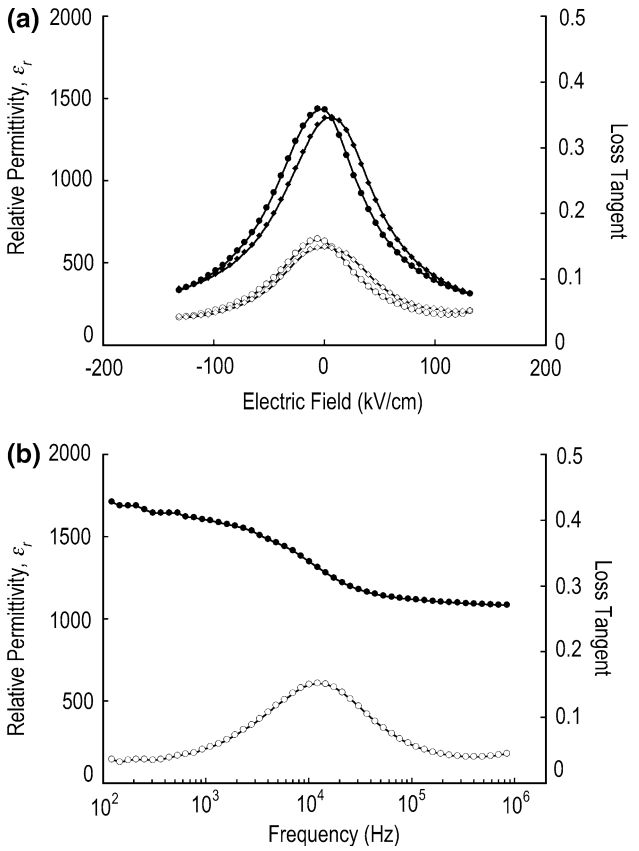

Fig. 6 (**a**) Field dependence and (**b**) frequency dependence of permittivity (solid markers) and loss tangent (open markers) for 100 ppm Mg-doped $BaTiO_3$ processed at 5×10^{-11} atm O_2

are shown in Fig. 6 for a Mg-doped sample fired in more oxidizing conditions. We begin to see an increase in the field dependent loss and a strong frequency dependent space charge contribution likely resulting from *p*-type compensation. The outcome of this experiment suggests one of the following possibilities: (1) The dopants are incorporated in the lattice and most or all are contributing to defect compensation such that increases in pO_2 produce *p*-type conductivity, or (2) The dopants are incorporated in the lattice at a lower level with additional dopant material phase-separated and not contributing to the overall defect equilibrium. Though both are possible, we have shown experimentally by electrical property analysis that higher dopant concentrations can be achieved for all cations tested [24]. If a solubility limit were present, the only effect would be more second phase at a volume fraction which provides negligible property impact. Consequently, we hypothesize that the dopants are dissolved into the $BaTiO_3$ lattice and are electrically active. This allows the assertion that oxygen vacancy levels can be inferred from the dopant concentration, which produces high insulation resistance and low dispersion in the absence of reoxidation annealing.

While doping was successful, the levels used are roughly three orders of magnitude greater than equilibrium calculations predict are needed for the firing conditions used. For example, using the bulk barium titanate reduction enthalpy, –567 kJ/mol, and assuming equilibration at the firing conditions, 350 ppb oxygen vacancies are expected; however, we compensate with 100,000 ppb acceptors [23]. A possible explanation is that these materials have higher overall vacancy concentrations than would be predicted using the bulk enthalpy values. A disparity between bulk and thin film defect chemistry may be expected given that bulk values were experimentally determined on materials with grain sizes in excess of 100 μm while the thin films are limited to approximately 100 nm [23]. The dramatic difference in grain boundary volume fraction cannot be ignored especially considering the potential for enhanced defect populations at crystalline surfaces. We suggest a composite vacancy model where the grain interiors exhibit the bulk reduction enthalpy, while the grain boundaries, where there is a greater degree of disorder, exhibit a reduced reduction enthalpy value. Subsequently, fine-grained materials with a much higher grain boundary volume fraction would be expected to have higher overall oxygen vacancy concentrations. This trend is consistent with that previously observed by Guo et al. [7] where the authors suggested a reduction enthalpy lowering in nano-scale $BaTiO_3$. We build upon their hypothesis by proposing a composite structure modification with the overall oxygen vacancy concentration being represented by two populations: those in the grain interior where a bulk-like reduction enthalpy largely dominates and those in the grain boundaries where the disordered structure results in a different reduction enthalpy as represented by Eq. (1). Here ΔH_{Bulk} and $\Delta H_{G.B.}$ are the bulk and grain boundary reduction enthalpies, respectively, R is the ideal gas constant, and x is the grain boundary volume fraction. As we are defining the oxygen vacancy concentration as site fractions, no pre-exponential constants are necessary [25]. It should be noted that the actual defect distribution in the grain boundary region has been shown to be heavily influenced by electrostatic contributions [26]. In this model, we do not discount this effect, rather we choose to focus on the grain boundary volume influence on the total defect population.

$$\left[V_{\mathrm{O}}^{x,\bullet,\bullet\bullet}\right] = (1 - x)\left[\frac{1}{4}\, pO_2^{-1/2} \exp\left(\frac{-\Delta H_{\mathrm{Bulk}}}{RT}\right)\right]^{1/3} + (x)\left[\frac{1}{4}\, pO_2^{-1/2} \exp\left(\frac{-\Delta H_{\mathrm{G.B.}}}{RT}\right)\right]^{1/3} \quad (1)$$

As a test for this model, we consider a barium titanate ceramic with 100 nm spherical grains and assume grain

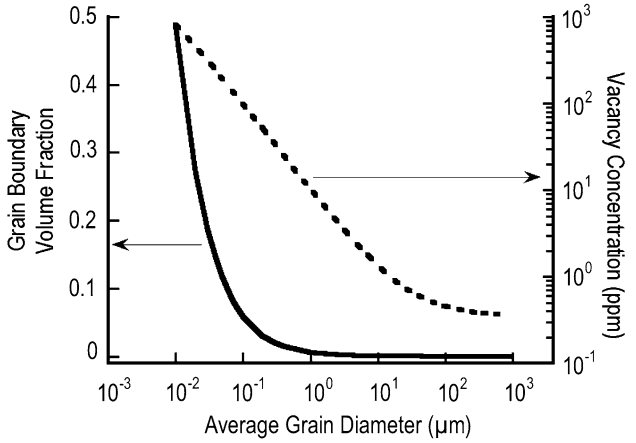

Fig. 7 Calculated grain size dependence of grain boundary volume fraction (solid line) and defect density (dashed line) for $BaTiO_3$ processed at 900 °C and 10^{-13} atm O_2

boundaries, two unit cells thick—a value that has been previously measured in well prepared fine-grained ceramics [27]. For 900 °C and 10^{-13} atm O_2 firing conditions we empirically identify from the dopant study that this material has defect densities of approximately 100 ppm. Using this concentration and these parameters, a calculated grain boundary volume fraction ($\sim$0.06 for 100 nm spherical grains with 2 unit cell thick boundaries), and the bulk reduction enthalpy, we can solve for a grain boundary reduction enthalpy of –402 kJ/mol using Eq. 1. This value represents a 30% reduction from the bulk and is consistent with the magnitude of property differences between crystal surfaces and interiors. This surface model and reduced-enthalpy value was applied to bulk materials with 100 μm grains. The effect on defect density is negligible, thus our hypothesis is consistent with both bulk and thin film materials. To illustrate this, a plot showing the grain boundary volume fraction and predicted defect concentration using our processing conditions versus average grain size is shown in Fig. 7 with the values calculated using our processing conditions and a two unit cell thick grain boundary. As seen in this figure, as grain sizes fall below 10 μm, the potential defect contribution from the grain interfaces are dramatic.

In summary, we have shown the feasibility of using acceptor dopants in barium titanate thin films processed under low pO_2 conditions to compensate for the intrinsic oxygen vacancies established by low oxygen partial pressure annealing. The necessary dopant levels necessary for high insulation resistance are orders of magnitude larger than predicted by existing models. To account for these differences a composite defect model consisting of bulk reduction enthalpies for grain interiors and reduced reduction enthalpies for grain surfaces was developed. An interface reduction enthalpy 30% lower than the bulk value will produce defect densities consistent with our experimental observations. This straightforward model illustrates the importance of surface contributions in nano-scaled ceramic materials and is relevant to many aspects of oxide thin film research.

Acknowledgements The authors wish to acknowledge the financial support of E. I. du Pont de Nemours and Company.

References

1. Dutta P, Pal S, Seehra MS, Shi Y, Eyring EM, Ernst RD (2006) Chem Mater 18:5144
2. Knauth P, Tuller HL (1999) J Appl Phys 85:897
3. Arlt G, Hennings D, De With G (1985) J Appl Phys 58:1619
4. Fong DD, Stephenson GB, Streiffer SK, Eastman JA, Auciello O, Fuoss PH, Thompson C (2004) Science 304:1650
5. McCauley D, Newnham RE, Randall CA (1998) J Am Ceram Soc 81:979
6. Parker CB, Maria JP, Kingon AI (2002) Appl Phys Lett 81:340
7. Guo X, Pithan C, Ohly C, Jia CL, Dornseiffer J, Haegel FH, Waser R (2005) Appl Phys Lett 86:082110
8. Dawley JT, Clem PG (2002) Appl Phys Lett 81:3028
9. Dawley JT, Ong RJ, Clem PG (2002) J Mater Res 17:1678
10. Ihlefeld J, Laughlin B, Hunt-Lowery A, Borland W, Kingon A, Maria J-P (2005) J Electroceram 14:95
11. Ihlefeld JF, Borland W, Maria J-P (2005) J Mater Res 10:2838
12. Laughlin B, Ihlefeld J, Maria JP (2005) J Am Ceram Soc 88:2652
13. Yang GY, Dickey EC, Randall CA, Barber DE, Pinceloup P, Henderson MA, Hill RA, Beeson JJ, Skamser DJ (2004) J Appl Phys 96:7492
14. Herbert JM (1963) Trans Brit Ceram Soc 62:645
15. Sakabe Y, Wada N, Hiramatsu T, Tonogaki T (2002) Jpn J Appl Phys, Part 1 41:6922
16. Burn I (1979) J Mater Sci 14:2453
17. Burn I, Maher GH (1975) J Mater Sci 10:633
18. Han YH, Appleby JB, Smyth DM (1987) J Am Ceram Soc 70:96
19. Barin I (1995) In: Thermochemical data of pure substances. VCH, Weinheim, New York
20. Murphy EJ, Morgan SO (1938) Bell Syst Tech J 17:640
21. Chan NH, Smyth DM (1976) J Electrochem Soc 123:1584
22. Chan NH, Sharma RK, Smyth DM (1981) J Am Ceram Soc 64:556
23. Chan NH, Sharma RK, Smyth DM (1982) J Am Ceram Soc 65:167
24. Ihlefeld JF (2006) Ph.D. Thesis, North Carolina State University
25. Smyth DM (2000) In: The defect chemistry of metal oxides. Oxford University Press, New York, pp 47
26. Waser R, Hagenbeck R (2000) Acta Mater 48:797
27. Frey MH, Xu Z, Han P, Payne DA (1998) Ferroelectrics 206:337